Proceedings of the European Conference Physics of Magnetism, Poznań 2014

Fragmentation of Co–Fe–Ta–B Soft Magnetic Amorphous Alloy

J. Mišкuf[a,*], K. Csach[a], A. Juríková[a], M. Huráková[a] and E.D. Tabachnikova[b]

[a]Institute of Experimental Physics, SAS, Watsonova 47, 040 01 Košice, Slovakia

[b]B. Verkin Institute for Low-temperature Physics and Engineering, UAS, Lenin ave. 47, Kharkov, Ukraine

The main limitation of high-strength Co-based bulk metallic glasses for their application as structural materials is the large brittleness. Spontaneously emerging cracks in the alloy degrade the magnetic properties. We analyzed the failure characteristics of $Co_{43}Fe_{20}Ta_{5.5}B_{31.5}$ bulk soft magnetic metallic glass deformed in the compression at room temperature and the low strain rate. Under loading the amorphous structure stores high elastic energy. During the failure this energy is released and the alloy breaks into small particles or powder exhibiting a fragmentation mode.

DOI: 10.12693/APhysPolA.127.558

PACS: 61.43.Dq, 62.25.Mn

1. Introduction

Cobalt based amorphous alloys exhibit unique magnetic properties (a combination of saturation magnetization, coercitive force, permeability, magnetostriction etc.) and have the high application potential. Proper modification of the composition of these alloys can enhance glass forming ability and enable to prepare these amorphous alloys named bulk metallic glasses (BMGs) in more suitable form. At the temperatures above the glass transition temperature they have the high deformation ability [1–3].

Shen et al. [4] developed the BMG with the composition of $Co_{43}Fe_{20}Ta_{5.5}B_{31.5}$ as an ultrahigh-strength material with the compressive true strength $\sigma_f = 5185$ MPa. Moreover, this alloy exhibits excellent soft magnetic properties (saturation magnetization of 0.3 T, low coercive force of 0.7 Am^{-1} and high effective permeability of 4×10^4 at 1 kHz).

High-strength BMGs usually exhibit the brittle behavior at the macroscopic level (like silicate glasses) whereas at the microscopic level they save the ductile behavior with necking and cavitation of viscous materials in liquid-like zone (obviously observed for metallic glasses) [5]. The plastic deformation of BMGs at room temperature is sustained by cooperative shearing of atomic clusters termed shear transformation zones (STZs) [6].

2. Experimental

The bulk amorphous alloy with the nominal composition of $Co_{43}Fe_{20}Ta_{5.5}B_{31.5}$ (at.%) in the form of cylinders with 2 and 3 mm in diameters were produced by an ejection of the melt into a copper mold. The cylinders cut from ingots were uniaxial loaded under the compression up to the failure. The amorphous structure of both the samples was confirmed by X-ray diffraction. The created fracture surfaces were examined using a high resolution scanning electron microscope.

3. Results and discussion

The form of prepared cylindric ingots is shown in Fig. 1a. After the compression both the cylinder samples broke into many fine fragments by bomb-like fracture [7]. At the macroscopic scale the failure is fragile in both cases. Under uniaxial compression, in the sites with locally enhanced free volume concentration the cracks initiate simultaneously [6]. The cracks propagate in all directions due to the complicated dynamic stresses conditions according to the scheme in Fig. 1b. The failure is only controlled by the applied stress without some preference orientations and does not follow the macroscopic shear planes [8–11].

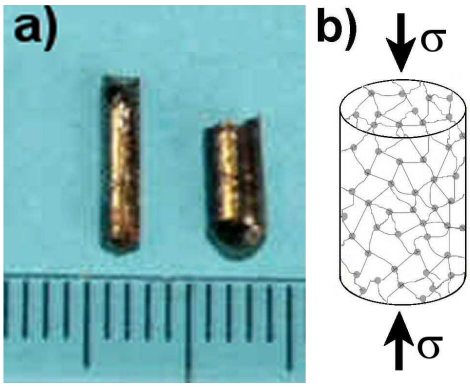

Fig. 1. The ingots of the prepared BMG (a) and the scheme of the fragmentation under uniaxial compression loading σ (b).

The elastic energy δ_E density stored in a BMG sample upon the failure can be expressed according to [12]:

$$\delta_E \sigma = \frac{\sigma_F^2}{2E},$$

*corresponding author; e-mail: miskuf@saske.sk

where E is Young's modulus and σ_F is the fracture strength of the BMG materials. In the case of high strength Co-based amorphous materials (about 5 GPa) the stored elastic energy is very high. At the high strength the cracks initiate at many small regions and samples fail into many fragments by the bomb-like failure process as Fig. 2a demonstrates. The elastic energy δ_E is used for the creation of new fracture surfaces.

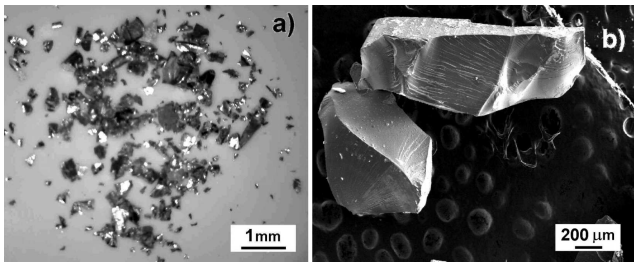

Fig. 2. The particles of a sample fragmented after the compression test (a) and the morphology of individual particles with the fracture surface (b).

Figure 2b shows the individual fragments after the failure. The individual particles have an irregular form with the fracture surfaces. The form of the fracture surface is conchoidal as can be seen in Fig. 3a. More cracks inside individual fragment are present in Fig. 3b.

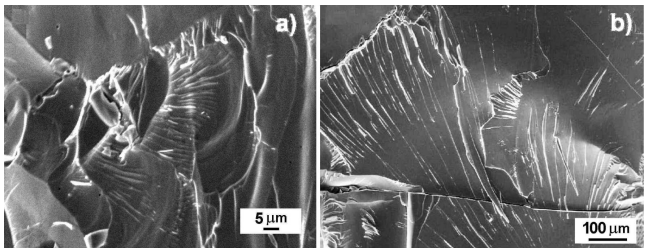

Fig. 3. The conchoidal fracture surface morphology with radiating cracks (a) and a detail of cracks inside of a single fragment propagated in different directions (b).

This fracture surface is divided by a crack in concurrent directions. On the fracture surface there can be identified the crack tip moving direction. Not all cracks tend to the particle decomposition necessary. The presence of cracks can degrade not only the mechanical but the magnetic properties, too [2].

The detailed observations of the fracture surface of the failed samples showed similarities in the micromorphology of the fracture surfaces of all observed fragments. Figure 4a shows the typical micromorphology of the failure surface covered by small uniform dimples.

This indicates the presence of plasticity in a narrow failure zone. The more radiating cracks originate from the tendency to flatten the originally conchoidal form of fracture surface into the shear plane. Rarely present microcrystalline regions (only in the sample with the diameter of 3 mm) have no principal influence on the main crack propagation as can be seen in Fig. 4b.

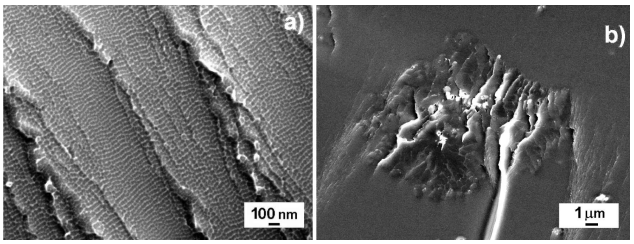

Fig. 4. Flat segments of a failure surface covered by periodically arranged dimples (a); an imperfection in a sample volume revealed by the failure process (b).

The investigation of magnetic properties in ultrahigh-strength $Co_{43}Fe_{20}Ta_{5.5}B_{31.5}$ bulk glassy alloy has shown that increase of the sample diameter up to 3 mm does not deteriorate the good soft magnetic properties [4].

A detail of the plane facette covered by nanoscaled dimples can be seen in Fig. 5a. The arrow indicates the crack front moving direction. Small (about 40 nm in size) dimples are arranged in periodic stripes perpendicular to the crack front. Strong rectangular distribution of dimples are in Fig. 5a. The hexagonal distribution of dimples observed in some small regions is marked by white circles. A detail of the hexagonal distribution with the schematic sketch is shown in Fig. 5b.

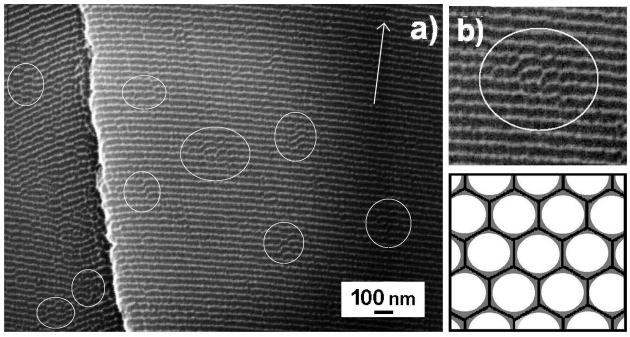

Fig. 5. A planar facette of failure with periodic arranged nanosized dimples, the arrow indicates the crack front moving direction (a); a detail of the hexagonal distribution of nanovoids with the corresponding sketch (b).

The nature of periodic arrangements of the voids is in the high velocity of crack front movements. Wang et al. [13] interpreted the regular void distribution respecting the periodic corrugations at the nanoscale level in brittle metallic glasses as a result of local dynamic softening mechanisms.

The period of corrugations (corresponding to the dimple size) was measured along the crack propagation direction. These values measured at the fracture surfaces for both samples in dependence of the corrugation distance from the edge of a particle are shown in Fig. 6. The edge of the particle was chosen as the zero value of the position.

For the estimation of characteristic period of corrugations L Jiang et al. [14] derived:

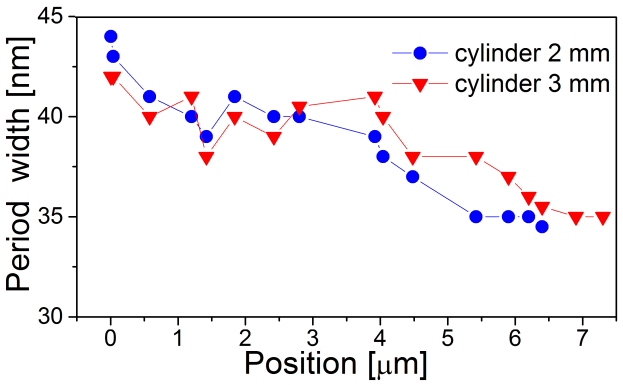

Fig. 6. The period width of the nanoscaled stripes along the crack propagation.

$$L = b\left(\frac{\sigma_{\rm th}}{\sigma_y}\right)^2,$$

where b is the tension transformation zone (TTZ) spacing, which is considered to be of the same order as the characteristic length size of a TTZ itself due to metallic glass' structural similarity to the "dense random packing of spheres" model [15]. Thus, b is less than 10 nm at a rough estimate. For high strength metallic glasses the yield strength σ_y reaches 10–50% value of the theoretical strength $\sigma_{\rm th}$. At these assumptions the characteristic period L of corrugation values can be calculated as $L = 100$ nm (or smaller).

Other possible interpretation of the periodic dimple morphology is based on the theoretical model of turbulent conditions of heat generation in front of the crack tip propagation [16]. Because the crack tip velocity is very high, the void distribution reflects the local temperature changes. The fracture surfaces contain the state of frozen-in conditions during the adiabatic shear band generation and failure.

4. Conclusion

The high strength bulk soft magnetic amorphous $Co_{43}Fe_{20}Ta_{5.5}B_{31.5}$ alloy exhibits macroscopic brittle behaviour under uniaxial compression. High stored elastic energy releases during the failure and the samples break into many fragments. Fracture surface morphology reflects the amorphous nature of the material. The failure is performed in a narrow region via local softening of the amorphous structure in the region in front of crack tips. In heated region inside the shear band, the homogeneous nucleation of voids via merging of free volume or STZs is present. The fracture surfaces consist from small (40 nm in diameter) dimples arranged in periodic corrugations. The corrugations are oriented perpendicular to the crack tip propagation direction.

Acknowledgments

This work was supported by the Slovak Academy of Sciences — VEGA 2/0045/14, by Slovak Research and Development Agency — contract No. APVV-0171-10 and by the project No. 26110230097 provided by the European Social Fund.

References

[1] H. Sun, Q. Man, Y. Dong, B. Shen, H. Kimura, A. Makino, A. Inoue, *J. Alloys Comp.* **504S**, S31 (2010).

[2] Ch.A. Schuh, T.C. Hufnagel, U. Ramamurty, *Acta Mater.* **55**, 4067 (2007).

[3] V. Ocelík, P. Diko, V. Hajko, J. Miskuf, P. Duhaj, *J. Mater. Sci.* **22**, 2305 (1987).

[4] B. Shen, A. Inoue, *J. Phys. Condens. Matter* **17**, 5647 (2005).

[5] Z.F. Zhang, F.F. Wu, W. Gao, J. Tan, Z.G. Wang, M. Stoica, J. Das, J. Eckert, B.L. Shen, A. Inoue, *Appl. Phys. Lett.* **89**, 251917 (2006).

[6] J.T. Fan, Z.F. Zhang, S.X. Mao, B.L. Shen, A. Inoue, *Intermetallics* **17**, 445 (2009).

[7] F.F. Wu, W. Zheng, S.D. Wu, Z.F. Zhang, J. Shen, *Int. J. Plastic.* **27**, 560 (2011).

[8] G. Wang, D.Q. Zhao, H.Y. Bai, M.X. Pan, A.L. Xia, B.S. Han, X.K. Xi, Y. Wu, W.H. Wang, *Phys. Rev. Lett.* **98**, 235501 (2007).

[9] W.Z. Liang, X.Y. Mao, L.Z. Wu, H.J. Yu, L. Zhang, *J. Mater. Sci.* **44**, 2016 (2009).

[10] Y.T. Wang, X.K. Xi, G. Wang, X.X. Xia, W.H. Wang, *J. Appl. Phys.* **106**, 13528 (2009).

[11] S. Brandt, J. Miskuf, D. Rautenbach, *J. Graph Theory* **57**, 333 (2008).

[12] Z.F. Zhang, H. Zhang, B.L. Shen, A. Inoue, J. Eckert, *Philos. Mag. Lett.* **86**, 10643 (2006).

[13] Y.T. Wang, X.K. Xi, G. Wang, X.X. Xia, W.H. Wang, *J. Appl. Phys.* **106**, 113528 (2009).

[14] M.Q. Jiang, Z. Ling, J.X. Meng, L.H. Dai, *Philos. Mag.* **88**, 407 (2008).

[15] D.J. Bernal *Nature (Lond.)* **185**, 68 (1960).

[16] X. Teng, T. Wierzbicki, H. Couque, *Mech. Mater.* **39**, 107 (2007).